Probe Position Errors Corrected Near-Field – Far-Field Transformation with Spherical Scanning

F. D'Agostino, F. Ferrara, C. Gennarelli, R. Guerriero, and M. Migliozzi

Dipartimento di Ingegneria Industriale
University of Salerno, via Giovanni Paolo II, 132 - 84084 Fisciano, Italy
fdagostino@unisa.it, flferrara@unisa.it, cgennarelli@unisa.it, rguerriero@unisa.it, mmigliozzi@unisa.it

Abstract ─ Two effective approaches to correct known positioning errors in a near-field – far-field (NF–FF) transformation with spherical scan for electrically long antennas are proposed and validated numerically and experimentally. They rely on a nonredundant sampling representation of the voltage acquired by the probe, obtained by assuming that the antenna under test is enclosed in a cylinder ended in two half-spheres. The former approach exploits the singular value decomposition method, to retrieve the NF data at the points fixed by the sampling representation from the acquired irregularly spaced ones, and can be used when the nonuniformly spaced samples lie on nonuniform parallels. The latter employs an iterative technique, which can be adopted even if such a hypothesis is not satisfied, but requires the existence of a one-to-one correspondence associating at each uniform sampling point, the nearest nonuniform one. Once the uniform samples have been recovered, the NF data needed by the classical spherical NF–FF transformation are efficiently evaluated via an optimal sampling interpolation algorithm.

Index Terms ─ Antenna measurements, nonredundant sampling representations, probe positioning errors compensation, spherical near-field – far-field transformation.

I. INTRODUCTION

Among the techniques which allow the evaluation of the antenna far field from measurements performed in the near-field region, the near-field – far-field (NF–FF) transformation with spherical scanning is the most interesting one, due to its unique features to allow the full reconstruction of the radiation pattern and to avoid the errors related to the truncation of the measurement surface. Therefore, it has attracted a considerable attention in the last four decades [1-15]. In fact, the first work dealing with a NF–FF transformation with spherical scanning based on the spherical wave expansion (SWE) was the Ph.D. dissertation thesis of Jensen [1], published later in a more complete form in the paper [2], wherein a proper transmission formula for the probe correction was derived. An efficient fast Fourier transform scheme to evaluate the SWE coefficients of the antenna under test (AUT) was then developed by Wacker [3], that also proposed the use of a probe with a pattern azimuthal dependence of the first order. Further improvements in the numerical efficiency were achieved in [4,5]. A comprehensive book [6], which deals with the theoretical as well as practical aspects of the classical probe-compensated NF–FF transformation with spherical scanning, was published by Hansen. Alternative probe-corrected formulas were derived in [7,8] by expressing the probe output in terms of the spatial derivatives of the incident field. Recently, the probe correction has been generalized to higher-order probes [9,10], thus allowing the characterization of wideband antennas without changing the probe.

The classical spherical NF–FF transformation [6] has been modified in [11], by taking into account the spatial bandlimitation properties of radiated electromagnetic (EM) fields [16]. In particular, the highest spherical wave to be considered has been fixed by these properties and the number of data on the parallels has resulted to be decreasing towards the poles. In this framework, the application of the nonredundant sampling representations of radiated EM fields [17,18] has allowed the development of effective NF–FF transformations with spherical scanning [11-14], which usually require a number of NF data remarkably lower than that needed by the classical one [6]. As a matter of fact, the NF data required by this last are accurately retrieved by interpolating a minimum set of measurements via optimal sampling interpolation (OSI) expansions. A remarkable measurement time saving can be so obtained making these nonredundant transformations more and more appealing, since today such a time is very much greater than the computational one needed to perform the transformation. This result relies on the fact that, according to the abovementioned representations, the EM fields radiated by antennas, enclosed in a convex domain bounded by a rotational surface Σ and observed on a surface M with the same rotational symmetry, can be very well approximated by spatially band-limited functions when a proper phase

Submitted On: July 2, 2015
Accepted On: November 3, 2015

factor is singled out from the field expression and proper parameterizations are adopted to describe M [17]. Since the voltage acquired by a nondirective probe has the same effective spatial bandwidth of the field radiated by the AUT, these representations can be applied to the voltage too. In particular, an elongated antenna has been considered as enclosed in a prolate ellipsoid [11,12] or in a rounded cylinder (a cylinder ended in two half-spheres) [13,14], whereas an oblate ellipsoid [11,12] or a double bowl (a surface formed by two circular bowls with the same aperture diameter, but with bending radii which can be different for a better fitting of the AUT geometry) [13,14] have been employed to model a quasi-planar antenna.

An alternative sampling technique for reducing the needed NF data has been developed in [15]. It makes use of a proper decision threshold to adaptively concentrate the acquisition on the strongly changing NF regions, while skipping the sampling points from the smoothly varying ones.

It must be stressed that the errors due to an imprecise control of the positioning systems and their finite resolution do not allow the exact placing of the probe at the points fixed by the sampling representation, even if their location can be accurately determined by optical devices. Therefore, it is very important to develop an effective algorithm for an accurate and stable reconstruction of the NF data needed by the NF–FF transformation from the irregularly spaced ones. To this end, an approach based on the conjugate gradient iteration method and exploiting the unequally spaced fast Fourier transform [19,20] has been developed for compensating the positioning errors in the classical NF–FF transformations with planar [21] and spherical [22] scannings. Unfortunately, such an approach is not tailored to the aforementioned nonredundant NF–FF transformations. A viable and convenient strategy [23] is to retrieve the uniform samples from the irregularly spaced (nonuniform) ones and then reconstruct the needed NF data via an accurate and stable OSI expansion. In this context, two different approaches have been proposed. The former is based on an iterative technique, which converges only if it is possible to build a biunique correspondence associating at each uniform sampling point the nearest nonuniform one, and has been applied to the reconstruction of the uniform samples in plane-rectangular [23], cylindrical and spherical grids [24]. The latter relies on the singular value decomposition (SVD) method, does not exhibit the above limitation and has been applied to the uniform samples reconstruction in planar [25,26] and cylindrical [27] geometries. It allows to exploit the data redundancy to increase the algorithm stability, but can be conveniently applied only if the uniform samples recovery can be reduced to the solution of two independent one-dimensional problems. At last, both the approaches have been applied and numerically compared in [28] with reference to the positioning errors compensation in the nonredundant spherical NF–FF transformation based on the prolate ellipsoidal AUT modelling.

The aim of this paper is to validate numerically and experimentally the application of these two approaches to the NF–FF transformation with spherical scanning for long antennas [13] using the rounded cylinder modelling (Fig. 1). The experimental tests have been carried out in the Antenna Characterization Lab of the University of Salerno, provided with a roll over azimuth spherical NF facility supplied by MI Technologies.

The nonredundant sampling representation on the scanning sphere for the voltage measured by the probe, obtained by modelling the AUT with a rounded cylinder, is summarized in Section 2. The two approaches to compensate known positioning errors are then presented in Section 3, and numerically and experimentally validated in Sections 4 and 5, respectively. Finally, the conclusions are drawn in Section 6.

II. NONREDUNDANT SAMPLING REPRESENTATION ON A SPHERE

Let us consider an electrically long AUT, enclosed in a convex domain $\mathcal{D}$ bounded by a surface Σ with rotational symmetry, a nondirective probe scanning a sphere of radius d in the antenna NF region, and adopt the spherical coordinate system (r,ϑ,φ) for denoting an observation point P (Fig. 1). Since the voltage measured by this type of probe has the same effective spatial bandwidth of the field radiated by the AUT, the nonredundant representations of EM fields [17] can be applied to obtain an effective sampling representation of it. Accordingly, it is convenient to adopt an optimal parameter ξ to describe each of the curves C (meridians and parallels) representing the sphere and to introduce the "reduced voltage":

$$\tilde{V}(\xi)=V(\xi)\mathrm{e}^{\mathrm{j}\gamma(\xi)}, \tag{1}$$

where $V(\xi)$ is the voltage V_1 or V_2 measured by the probe or by the rated probe, and $\gamma(\xi)$ is a proper phase function to be determined. The error, occurring when $\tilde{V}(\xi)$ is approximated by a bandlimited function, becomes negligible as the bandwidth exceeds a critical value W_ξ [17] and can be effectively controlled by considering approximating functions with bandwidth $\chi' W_\xi$, where $\chi'>1$ is the enlargement bandwidth factor, slightly greater than unity for electrically large antennas. As shown in [13], an effective modelling for an elongated antenna is obtained by assuming a rounded cylinder as surface Σ enclosing it, namely, a cylinder of height h' ended in two half-spheres of radius a' (see Figs. 1 and 2).

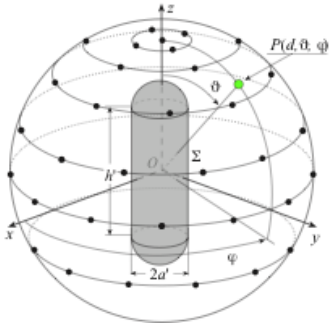

Fig. 1. Spherical scanning for a long antenna.

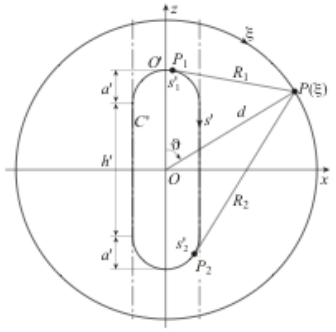

Fig. 2. Relevant to the rounded cylinder modelling.

When considering a meridian, the bandwidth W_ξ, the parameterization ξ and the corresponding phase function γ are [13,17]:

$$W_\xi = \beta \ell' / 2\pi, \tag{2}$$

$$\gamma = (\beta/2)\left[R_1 + R_2 + s_1' - s_2'\right], \tag{3}$$

$$\xi = (\pi/\ell')\left[R_1 - R_2 + s_1' + s_2'\right], \tag{4}$$

where β is the wavenmumber, $\ell' = 2(h' + \pi a')$ is the length of the intersection curve C' between the meridian plane through the observation point P and Σ, $R_{1,2}$ are the distances from P to the two tangency points $P_{1,2}$ between the cone of vertex at P and C', and $s_{1,2}'$ are their curvilinear abscissae (see Fig. 2). The explicit expressions of $R_{1,2}$ and $s_{1,2}'$, which change depending on the location of the points $P_{1,2}$, have been determined in [13] and are reported below for reader's convenience. In particular, three cases occur when ϑ varies in the angular range [0, π] (see Fig. 2).

For $0 \le \vartheta \le \sin^{-1}(a'/d)$, it results:

$$R_1 = \sqrt{(d\sin\vartheta)^2 + (d\cos\vartheta - h'/2)^2 - a'^2}, \tag{5}$$

$$s_1' = a'\sin^{-1}\left(\frac{a'd\sin\vartheta + R_1(h'/2 - d\cos\vartheta)}{R_1^2 + a'^2}\right), \tag{6}$$

$$s_2' = a'\sin^{-1}\left(\frac{a'd\sin\vartheta - R_2(h'/2 - d\cos\vartheta)}{R_2^2 + a'^2}\right), \tag{7}$$

and $R_2 = R_1$.

For $\sin^{-1}(a'/d) < \vartheta \le \pi - \sin^{-1}(a'/d)$, R_1 and s_1' are given by (5) and (6), while:

$$R_2 = \sqrt{(d\sin\vartheta)^2 + (d\cos\vartheta + h'/2)^2 - a'^2}, \tag{8}$$

$$s_2' = h' + a'\left[\pi - \sin^{-1}\left(\frac{a'd\sin\vartheta + R_2(h'/2 + d\cos\vartheta)}{R_2^2 + a'^2}\right)\right]. \tag{9}$$

Finally, when $\pi - \sin^{-1}(a'/d) < \vartheta \le \pi$, R_2 and s_2' are again given by (8) and (9), whereas:

$$R_1 = \sqrt{(d\sin\vartheta)^2 + (d\cos\vartheta + h'/2)^2 - a'^2}, \tag{10}$$

$$s_1' = h' + a'\left[\frac{\pi}{2} - \sin^{-1}\left(\frac{R_1 d\sin\vartheta + a'(h'/2 + d\cos\vartheta)}{R_1^2 + a'^2}\right)\right], \tag{11}$$

when C is a parallel, the phase function is constant and it is convenient to use the azimuthal angle φ as parameter. The related bandwidth W_φ is given [13,17] by:

$$W_\varphi = \frac{\beta}{2}\max_{z'}(R^+ - R^-) = \frac{\beta}{2}\max_{z'}\left(\sqrt{(z-z')^2 + (\rho + \rho'(z'))^2} - \sqrt{(z-z')^2 + (\rho - \rho'(z'))^2}\right), \tag{12}$$

wherein $\rho = d\sin\vartheta$, $\rho'(z')$ is the equation of Σ in cylindrical coordinates and the maximum is achieved [13] at:

$$z' = \begin{cases} z & |z| \le h'/2 \\ \left[\dfrac{h'}{2} + \dfrac{(|z| - h'/2)\ a'^2}{(d\sin\vartheta)^2 + (|z| - h'/2)^2}\right]\mathrm{sgn}(z) & |z| > h'/2 \end{cases}, \tag{13}$$

$\mathrm{sgn}(\cdot)$ being the sign function.

According to the above results, the reduced voltage at P on the meridian at φ can be efficiently reconstructed by means of the OSI expansion [13]:

$$\tilde{V}(\xi(\vartheta), \varphi) = \sum_{n=n_0-q+1}^{n_0+q} \tilde{V}(\xi_n, \varphi)\, G\left(\xi, \xi_n, \bar{\xi}, N, N''\right), \tag{14}$$

where $n_0 = \mathrm{Int}(\xi/\Delta\xi)$, $2q$ is the number of retained intermediate samples $\tilde{V}(\xi_n, \varphi)$, i.e., the reduced voltages at the intersection points between the sampling parallels and the meridian passing through P:

$$G\left(\xi, \xi_n, \bar{\xi}, N, N''\right) = \Omega_N\left(\xi - \xi_n, \bar{\xi}\right) D_{N''}(\xi - \xi_n), \tag{15}$$

$$\xi_n = n\Delta\xi = 2\pi n/(2N''+1);\ N'' = \mathrm{Int}(\chi N') + 1, \tag{16}$$

$$N' = \mathrm{Int}(\chi' W_\xi) + 1;\ N = N'' - N';\ \bar{\xi} = q\Delta\xi, \tag{17}$$

χ being an oversampling factor controlling the truncation error [17] and Int(x) denoting the integer part of x. In (15),

$$D_{N''}(\xi)=\frac{\sin[(2N''+1)\xi/2]}{(2N''+1)\sin(\xi/2)}, \quad (18)$$

$$\Omega_N(\xi,\bar{\xi})=\frac{T_N\left[2\cos^2(\xi/2)/\cos^2(\bar{\xi}/2)-1\right]}{T_N\left[2/\cos^2(\bar{\xi}/2)-1\right]}, \quad (19)$$

are the Dirichlet and Tschebyscheff sampling functions [17], $T_N(\vartheta)$ being the Tschebyscheff polynomial of degree N. The intermediate samples are given by [13]:

$$\tilde{V}(\xi_n,\varphi)=\sum_{m=m_0-p+1}^{m_0+p}\tilde{V}(\xi_n,\varphi_{m,n})G(\varphi,\varphi_{m,n},\bar{\varphi},M_n,M_n''), \quad (20)$$

wherein $m_0=\mathrm{Int}(\varphi/\Delta\varphi_n)$, $2p$ is the retained samples number, $\tilde{V}(\xi_n,\varphi_{m,n})$ are the reduced voltage samples on the parallel fixed by ξ_n, and

$$\varphi_{m,n}=m\Delta\varphi_n=2\pi m/(2M_n''+1);\ M_n''=\mathrm{Int}(\chi M_n')+1, \quad (21)$$

$$M_n'=\mathrm{Int}\left[\chi^* W_\varphi(\xi_n)\right]+1;\ \ M_n=M_n''-M_n', \quad (22)$$

$$\chi^*=1+(\chi'-1)\left[\sin\vartheta(\xi_n)\right]^{-2/3};\ \bar{\varphi}=p\Delta\varphi_n. \quad (23)$$

The accurate reconstruction of the voltages V_1 and V_2 at any point on the sphere can be then obtained by matching the OSI expansions (14) and (20).

III. FROM NONUNIFORM TO UNIFORM SAMPLES

Two different approaches to correct known positioning errors are presented in this section by highlighting their advantages and limitations. These approaches are then numerically and experimentally validated in Sections 4 and 5, respectively.

A. The SVD-based approach

Let us suppose that, apart the sample at the pole $\vartheta=0$, the irregularly spaced samples lie on parallels not uniformly distributed on the scanning sphere, which represents a realistic hypothesis in a spherical NF facility, when the NF data are acquired by scanning along parallels as it is required to exploit the possibility to reduce the number of NF data on the noncentral parallels, offered by the previous nonredundant representation. In this case, the uniform samples recovery reduces to the solution of two independent one-dimensional problems.

The uniform $2M_k''+1$ samples on a nonuniform parallel at $\vartheta(\eta_k)$ are recovered as follows. Given a sequence of $J_k \geq 2M_k''+1$ nonuniform sampling points (η_k,ϕ_j) on such a parallel, the related reduced voltages $\tilde{V}(\eta_k,\phi_j)$ can be expressed in terms of the uniform ones by means of (20), thus getting a linear system which can be rewritten in the matrix form:

$$\underline{\underline{A}}\,\underline{x}=\underline{b}, \quad (24)$$

where $\underline{x}$ is the vector of the unknown uniform samples $\tilde{V}(\eta_k,\varphi_{m,k})$, $\underline{b}$ is that of the known nonuniform ones $\tilde{V}(\eta_k,\phi_j)$, and $\underline{\underline{A}}$ is a $J_k\times(2M_k''+1)$ matrix, whose elements:

$$a_{jm}=G\left(\phi_j,\varphi_{m,k},\bar{\varphi}_k,M_k,M_k''\right), \quad (25)$$

are the weight functions of the OSI expansion, where $\varphi_{m,k}=m\Delta\varphi_k=2m\pi/(2M_k''+1)$ and $\bar{\varphi}_k=p\Delta\varphi_k$. It is useful to note that, for a fixed row j, the elements a_{jm} are zero if the index m is external to the range $[m_0(\phi_j)-p+1,\ m_0(\phi_j)+p]$. The SVD method is then applied to get the best least square approximated solution of (24). After this step, the OSI expansion (20), where the samples $\tilde{V}(\eta_k,\varphi_{m,k})$ take the role of the $\tilde{V}(\xi_n,\varphi_{m,n})$ ones, is employed to determine the intermediate samples $\tilde{V}(\eta_k,\varphi)$ at the intersection points between the nonuniform parallels and the meridian through P. Since these samples are again irregularly spaced, the voltage at P can be found by first recovering the uniformly distributed intermediate samples $\tilde{V}(\xi_n,\varphi)$ again via SVD and then interpolating them by means of the OSI expansion (14).

Both the distances between each nonuniform parallel and the related uniform one and those between the nonuniform sampling points and the associated uniform ones on the nonuniform parallels have been assumed less than one half of the corresponding uniform spacing to avoid a strong ill-conditioning of the related linear systems.

It must be stressed that it is convenient to retrieve the same number N_φ of uniform samples on each nonuniform parallel to minimize the computational effort. In fact, in such a case, these samples are aligned along the meridians and, accordingly, the number of systems to be solved is minimum. Obviously, the number N_φ is that corresponding to the equator, wherein the azimuthal bandwidth W_φ attains its maximum value. Once the uniform samples have been determined, the data needed by the standard NF–FF transformation [6] can be evaluated by means of the OSI expansions (14) and (20), this last properly modified to account for the redundancy in φ.

The SVD-based approach could be still used when the irregularly spaced samples no longer lie on parallels, but the dimension of the involved matrix would become very large, thus requiring a huge computational effort. Accordingly, in such a case, it is more convenient [28] to resort to the iterative technique, which will be described in the next subsection.

B. The iterative approach

Let us now suppose that, save for the sample at the pole $\vartheta = 0$, all the others are irregularly spaced on the scanning sphere. Moreover, let us assume that the nonuniform samples distribution is such that it is possible to build a biunique correspondence between each uniform sampling point and the "nearest" nonuniform one. By expressing the reduced voltage at each nonuniform sampling point $(\eta_k, \phi_{j,k})$ as a function of the unknown values at the nearest uniform ones $(\xi_n, \varphi_{m,n})$ by means of the OSI expansions (14) and (20), we obtain:

$$\tilde{V}(\eta_k, \phi_{j,k}) = \sum_{n=n_0-q+1}^{n_0+q} \left\{ G(\eta_k, \xi_n, \bar{\xi}, N, N'') \cdot \sum_{m=m_0-p+1}^{m_0+p} \tilde{V}(\xi_n, \varphi_{m,n})\, G(\phi_{j,k}, \varphi_{m,n}, \bar{\varphi}, M_n, M_n'') \right\}. \quad (26)$$

The resulting linear system can be rewritten in the form $\underline{\underline{A}}\,\underline{x} = \underline{b}$, where b is the vector of the known nonuniform samples $\tilde{V}(\eta_k, \phi_{j,k})$, $\underline{x}$ is that of the unknown uniform ones $\tilde{V}(\xi_n, \varphi_{m,n})$, and $\underline{\underline{A}}$ is a sparse banded matrix of sizes $Q \times Q$, wherein Q is the overall number of uniform/nonuniform samples. By splitting the matrix $\underline{\underline{A}}$ into its diagonal part $\underline{\underline{A}}_D$ and nondiagonal one $\underline{\underline{\Delta}}$, multiplying both members of the system by $\underline{\underline{A}}_D^{-1}$ and rearranging the terms, the following iterative procedure results:

$$\underline{x}^{(\nu)} = \underline{\underline{A}}_D^{-1}\underline{b} - \underline{\underline{A}}_D^{-1}\underline{\underline{\Delta}}\,\underline{x}^{(\nu-1)} = \underline{x}^{(0)} - \underline{\underline{A}}_D^{-1}\underline{\underline{\Delta}}\,\underline{x}^{(\nu-1)}, \quad (27)$$

$\underline{x}^{(\nu)}$ being the uniform samples vector estimated at the νth step. The necessary conditions for the convergence of the procedure are surely fulfulled in the assumed hypothesis on the nonuniform samples distribution. In fact, the modulus of each element on the principal diagonal of $\underline{\underline{A}}$ results to be not zero and greater than those of the other elements on the same row and column. In explicit form, Eq. (27) becomes:

$$\tilde{V}^{(\nu)}(\xi_n, \varphi_{m,n}) = \frac{1}{G(\eta_n, \xi_n, \bar{\xi}, N, N'')\, G(\phi_{m,n}, \varphi_{m,n}, \bar{\varphi}, M_n, M_n'')} \cdot \left\{ \tilde{V}(\eta_n, \phi_{m,n}) - \sum_{\substack{\ell=\ell_0-q+1 \\ (\ell \neq n)}}^{\ell_0+q} \sum_{\substack{i=i_0-p+1 \\ \wedge\ (i \neq m)}}^{i_0+p} G(\eta_n, \xi_\ell, \bar{\xi}, N, N'') \cdot G(\phi_{m,n}, \varphi_{i,\ell}, \bar{\varphi}, M_\ell, M_\ell'')\, \tilde{V}^{(\nu-1)}(\xi_\ell, \varphi_{i,\ell}) \right\}. \quad (28)$$

Once the regularly spaced samples have been recovered, the NF data needed by the standard NF–FF transformation [6] can be determined via the OSI expansions (14) and (20).

IV. SIMULATION RESULTS

Some numerical results, which assess the effectiveness of the described approaches to correct known positioning errors in the NF–FF transformation with spherical scanning using the rounded cylinder modelling of the antenna, are shown in this section. The simulations, which complete the preliminary ones reported in [29], are relevant to a uniform planar array of elementary Huygens sources polarized along the *z* axis, spaced by 0.5λ (λ being the wavelength), which cover a zone in the plane $y = 0$, formed by a rectangle ended in two half-circles. The sizes of the rectangle are: $2a' = 14\lambda$ and $h' = 40\lambda$. The scanning sphere has radius $d = 35\lambda$ and an open-ended circular waveguide, having radius 0.338λ, is chosen as probe.

The first set of simulations (from Fig. 3 to Fig. 6) is relevant to the case of irregularly distributed samples lying on parallels nonuniformly spaced on the scan sphere, so that the reconstruction of the uniform samples can be split into the solution of two independent one-dimensional problems. The nonuniform samples have been generated by imposing that the distances in ξ and φ between each nonuniform parallel and the related uniform one and those between the nonuniform sampling points and the associated uniform ones on the nonuniform parallels are random variables uniformly distributed in $(-\Delta\xi/2, \Delta\xi/2)$ and $(-\Delta\varphi_k/2, \Delta\varphi_k/2)$, which is a pessimistic hypothesis in an actual scanning system. Figures 3 and 4 show the reconstruction of the amplitude of the rotated probe voltage V_2 on the meridians at $\varphi = 0°$ and $\varphi = 90°$, respectively. As can be seen, the reconstruction is everywhere accurate, thus assessing the accuracy of the approach. For completeness, the reconstruction of the phase of V_2 on the meridian $\varphi = 90°$ is also reported in Fig. 5. To assess in a more quantitative way the algorithm performances, the mean-square errors in the reconstruction of the uniform samples of V_2 have been evaluated. They are normalized to the voltage maximum value on the sphere and have been obtained by comparing the recovered and the exact uniform samples. Figure 6 shows these errors for $\chi = 1.15, 1.20, 1.25$, $\chi' = 1.20$ and $p = q$ ranging from 2 to 12. Practical identical results, non-reported here to save space, have been obtained by applying the iterative algorithm to the same set of irregularly spaced NF data, which fulfils also its applicability conditions.

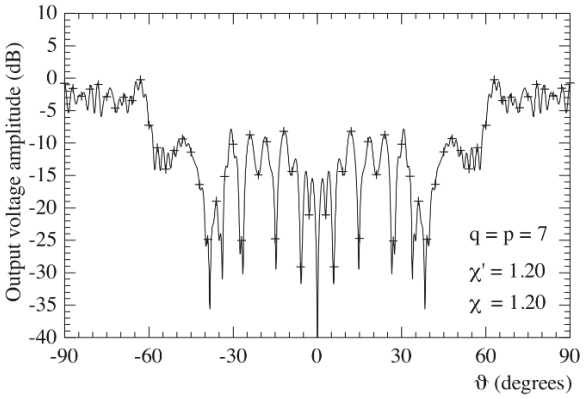

Fig. 3. Amplitude of V_2 on the meridian at $\varphi = 0°$. Solid line: exact. Crosses: reconstructed from nonuniform samples via the SVD-based algorithm.

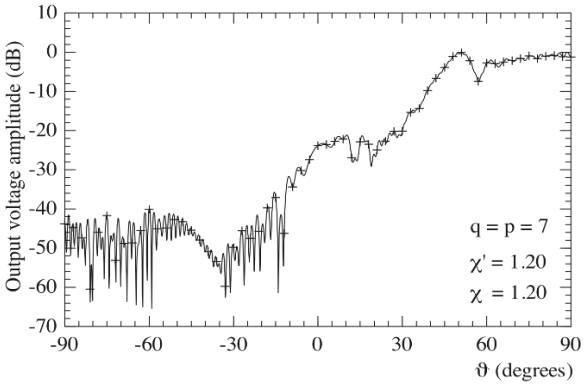

Fig. 4. Amplitude of V_2 on the meridian at $\varphi = 90°$. Solid line: exact. Crosses: reconstructed from nonuniform samples via the SVD-based algorithm.

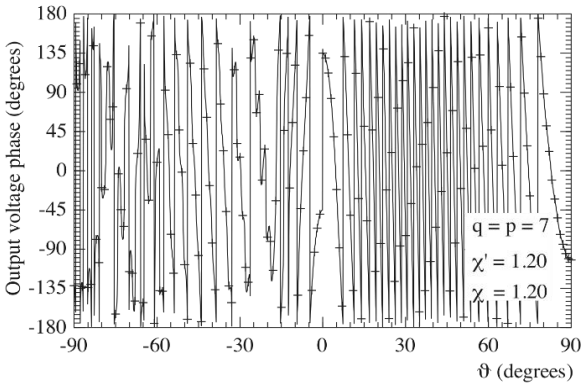

Fig. 5. Phase of V_2 on the meridian at $\varphi = 90°$. Solid line: exact. Crosses: reconstructed from nonuniform samples via the SVD-based algorithm.

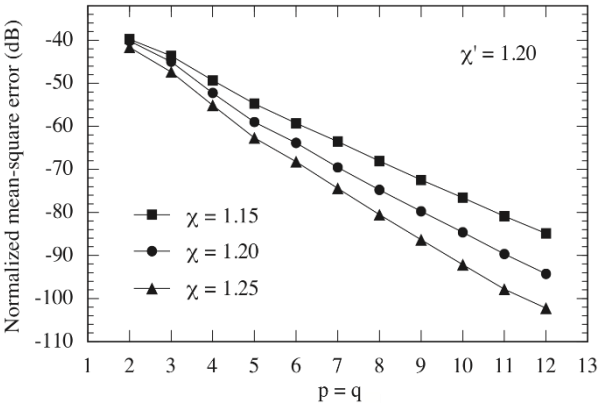

Fig. 6. Normalized mean-square errors in the reconstruction of the uniform samples of V_2 via the SVD-based algorithm.

The second set of numerical tests refers to the case of samples irregularly spaced on the sphere, which do not lie on parallels. In such a situation, it is more convenient, from the computational point of view, to employ the iterative algorithm, which requires the existence of a biunique correspondence between the uniform and nonuniform samples, that associates at each uniform sampling point the nearest irregular one. Therefore, the nonuniform samples have been generated in such a way that the displacements in ξ and φ between each nonuniform sampling point and the corresponding uniform one are random variables uniformly distributed in $(-\Delta\xi/3, \Delta\xi/3)$ and $(-\Delta\varphi_n/3, \Delta\varphi_n/3)$. To assess the effectiveness of the iterative algorithm, the normalized mean-square errors in the reconstruction of the uniform samples of V_2 have been evaluated. They are shown in Table 1 as function of the number of iterations ν and retained samples number $p = q$. As can be seen, these errors decrease on increasing ν and $p = q$. Moreover, just few iterations are enough to ensure the convergence of the iterative scheme.

Once the regularly spaced (uniform) samples have been retrieved by applying the SVD-based approach or the iterative one, depending on the considered nonuniform samples distribution, they have to be interpolated to reconstruct the NF data required by the classical spherical NF–FF transformation. Figures 7 and 8 show the comparison between the exact far field patterns in the principal planes and those obtained from the former set of irregularly spaced samples via the SVD-based algorithm and from the latter by applying the iterative approach. As can be seen, a very good reconstruction results.

Table 1: Normalized mean-square errors in the reconstruction of the uniform samples of V_2 versus the number of iterations and the retained samples number

p = q \ # iterations (ν)	0	1	2	3	4	5	6	7	8	9	10
3	-33.08	-46.24	-48.50	-48.53	-48.53	-48.53	-48.53	-48.53	-48.53	-48.53	-48.53
4	-32.96	-48.72	-54.64	-54.94	-54.95	-54.95	-54.95	-54.95	-54.95	-54.95	-54.95
5	-32.89	-49.31	-60.10	-61.25	-61.26	-61.26	-61.26	-61.26	-61.26	-61.26	-61.26
6	-32.87	-49.28	-63.15	-66.41	-66.51	-66.51	-66.52	-66.52	-66.52	-66.52	-66.52
7	-32.87	-49.21	-64.60	-71.48	-71.88	-71.89	-71.89	-71.89	-71.89	-71.89	-71.89
8	-32.86	-49.12	-65.06	-75.95	-77.28	-77.31	-77.31	-77.31	-77.31	-77.31	-77.31
9	-32.86	-49.04	-65.07	-78.72	-82.16	-82.31	-82.31	-82.31	-82.31	-82.31	-82.31
10	-32.85	-48.96	-64.99	-80.14	-86.98	-87.38	-87.39	-87.39	-87.39	-87.39	-87.39
11	-32.84	-48.90	-64.87	-80.62	-91.11	-92.39	-92.42	-92.42	-92.42	-92.42	-92.42
12	-32.84	-48.84	-64.76	-80.65	-94.12	-97.07	-97.16	-97.17	-97.17	-97.17	-97.17

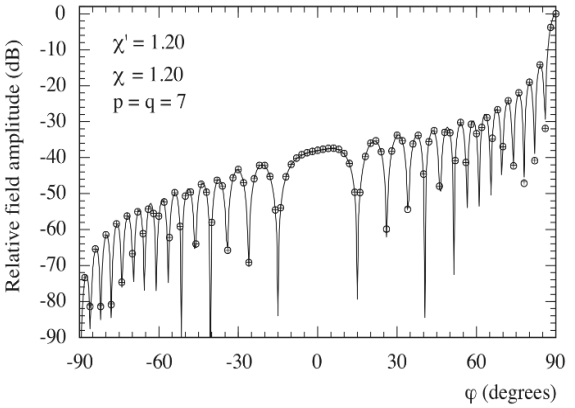

Fig. 7. H-plane pattern. Solid line: exact. Crosses: reconstructed from nonuniform samples (first set) via the SVD-based algorithm. Circles: reconstructed from nonuniform samples (second set) via the iterative approach.

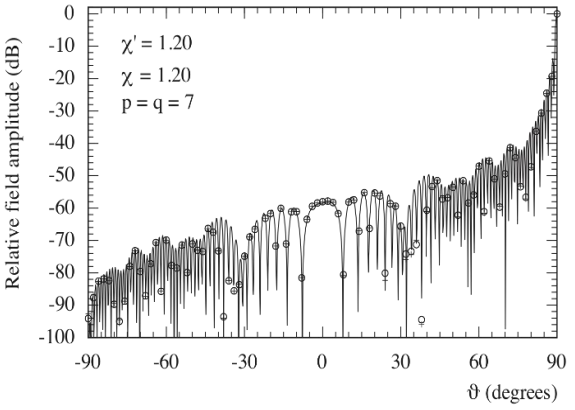

Fig. 8. E-plane pattern. Solid line: exact. Crosses: reconstructed from nonuniform samples (first set) via the SVD-based algorithm. Circles: reconstructed from nonuniform samples (second set) via the iterative approach.

It must be stressed that the reconstructions would be severely compromised without using these positioning errors compensation techniques, see, for instance, Fig. 9, which shows the corresponding reconstructed E-plane pattern, obtained from the second set of irregularly spaced NF data without using the iterative approach.

It can be interesting to compare the number of the used nonuniform NF data (19 489) with those (130 562) needed by the classical NF–FF transformation with spherical scanning [6].

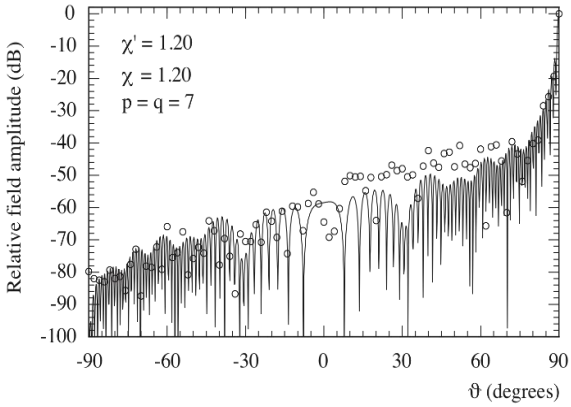

Fig. 9. E-plane pattern. Solid line: exact. Circles: reconstructed from nonuniform samples (second set) without using the iterative approach.

V. EXPERIMENTAL RESULTS

The described techniques have been experimentally tested in the anechoic chamber of the Antenna Characterization Lab of the University of Salerno, wherein a roll (φ axis) over azimuth (ϑ axis) spherical NF facility, supplied by MI Technologies, is available. The chamber, $8\text{m}\times5\text{m}\times4\text{m}$ sized, is covered with pyramidal absorbers which ensure a wall reflectivity lower than –40 dB. The measurements are

carried out by means of a vector network analyzer. The reported experimental results refer to a X-band resonant slotted waveguide array made by PROCOM A/S, which works at 10.4 GHz and has been realized by cutting 12 round-ended slots on both the broad walls of a WR-90 rectangular waveguide and soldering two cylinders on its narrow walls (see Fig. 10). Such an antenna has been modelled by a rounded cylinder with $h' = 28.27$ cm, $a' = 2.60$ cm and mounted in such a way that the broad walls are parallel to the plane $y = 0$ and its axis is coincident with the z one (Fig. 1). The probe voltages have been collected by an open-ended WR-90 waveguide on a sphere with radius $d = 45.20$ cm.

The first set of figures (from Fig. 11 to Fig. 16) is relevant to the case of the irregularly spaced sampling points lying on parallels of the scanning sphere. The NF data have been collected in such a way that the distances between each nonuniform parallel and the related uniform one and between the nonuniform sampling points and the uniform ones on the nonuniform parallels are random variables uniformly distributed in $(-\Delta\xi/2, \Delta\xi/2)$ and $(-\Delta\varphi_k/2, \Delta\varphi_k/2)$, respectively. The amplitude and phase of the probe voltage V_1 on the meridian at $\varphi = 0°$, recovered via the SVD-based approach, are compared in Figs. 11 and 12 with those directly measured on the same meridian. As can be seen, the reconstructions are very accurate, in spite of the severe values of the positioning errors.

The overall effectiveness of the SVD-based technique is assessed by comparing the FF patterns in the principal planes E and H (Figs. 13 and 14) reconstructed from the nonuniform NF data with those (references) obtained from the NF data directly acquired on the classical spherical grid. In both the cases, the MI Technologies' software MI-3000, implementing the classical spherical NF–FF transformation [6], has been used to obtain the FF reconstructions. The FF pattern reconstruction in the cut plane at $\varphi = 90°$ is then shown in Fig. 15. Also the FF reconstructions result to be very accurate, thus confirming the effectiveness of the approach. Practical identical results (non-reported for space saving) have been obtained by applying the iterative approach to the same set of nonuniform NF data, which satisfies also its applicability conditions. It is useful to note that the number of used samples is 836, remarkably less than that (5 100) required by the standard NF–FF transformation [6]. At last, the FF pattern in the cut plane at $\varphi = 90°$, reconstructed from the collected irregularly spaced NF data without using the SVD-based approach, is shown in Fig. 16. As can be seen, this FF reconstruction is severely compromised as compared with those achieved by using the proposed techniques, thus further confirming their capability to effectively compensate known positioning errors. The remaining figures (from Fig. 17 to Fig. 20) are relevant to the case of sampling points irregularly spaced on the sphere which do not lie on parallels and, therefore, only the iterative technique can be conveniently applied. The nonuniform samples have been acquired in such a way that the displacements in ξ and φ between the position of each nonuniform sample and that of the associated uniform one are random variables uniformly distributed in $(-\Delta\xi/3, \Delta\xi/3)$ and $(-\Delta\varphi_n/3, \Delta\varphi_n/3)$. The amplitude and phase of the voltage V_1 on the meridian at $\varphi = 0°$ recovered by using 10 iterations are compared in Figs. 17 and 18 with those directly measured on the same meridian. It must be stressed that such a number of iterations ensures the convergence of the algorithm with very low errors. At last, the overall effectiveness of the iterative technique is confirmed by the E-plane and H-plane pattern reconstructions reported in Figs. 19 and 20.

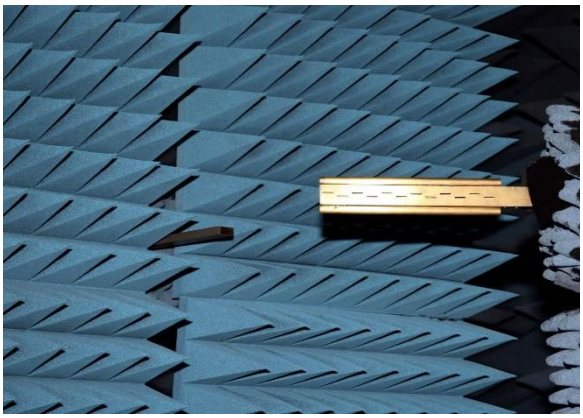

Fig. 10. Photo of the X-band resonant slotted waveguide array.

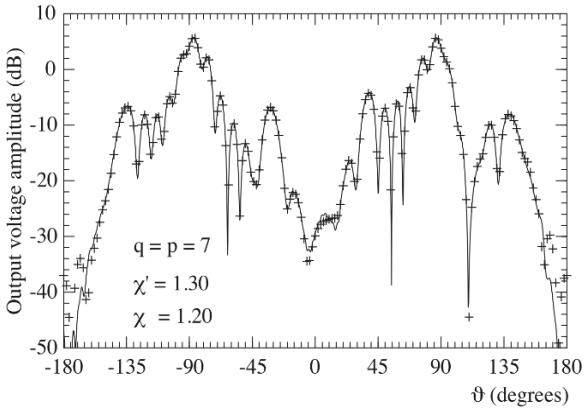

Fig. 11. Amplitude of V_1 on the meridian at $\varphi = 0°$. Solid line: measured. Crosses: reconstructed from nonuniform NF data via the SVD-based algorithm.

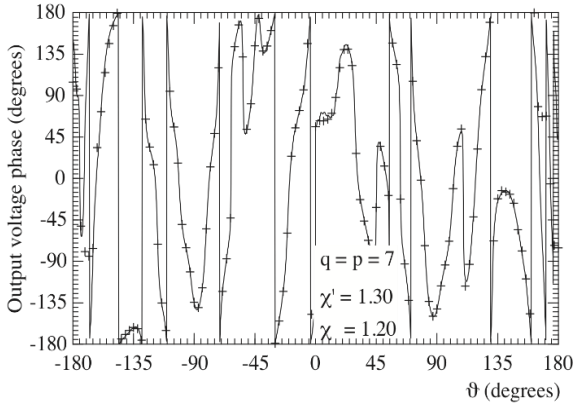

Fig. 12. Phase of V_1 on the meridian at $\varphi = 0°$. Solid line: measured. Crosses: reconstructed from nonuniform NF data via the SVD-based algorithm.

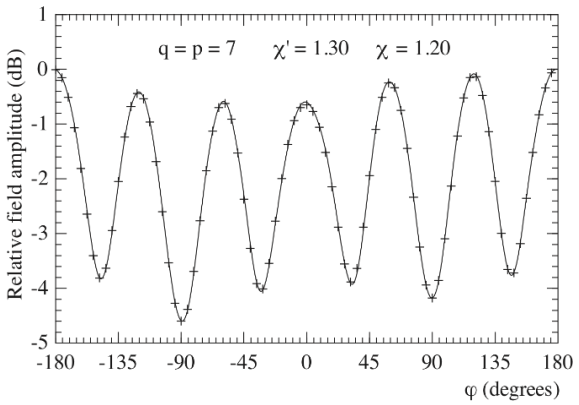

Fig. 13. E-plane ($\vartheta = 90°$) pattern. Solid line: reference. Crosses: reconstructed from nonuniform NF data via the SVD-based algorithm.

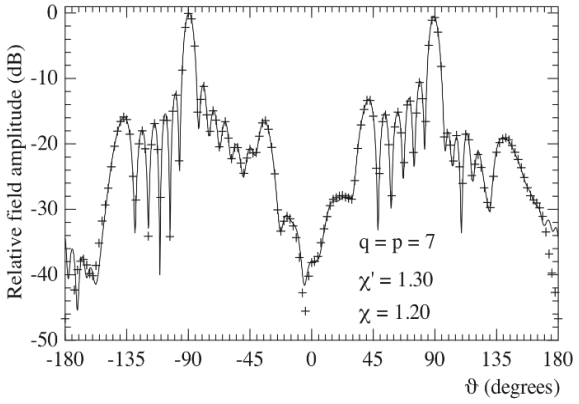

Fig. 14. H-plane ($\varphi = 0°$) pattern. Solid line: reference. Crosses: reconstructed from nonuniform NF data via the SVD-based algorithm.

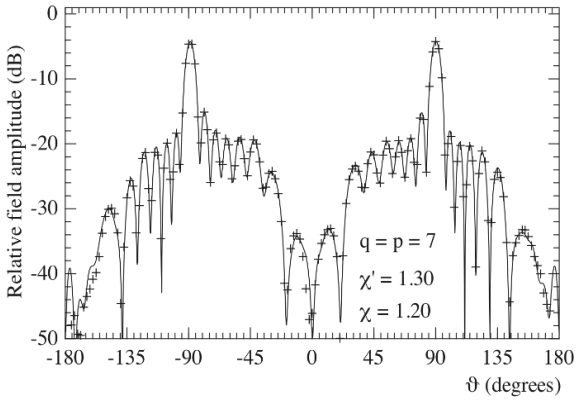

Fig. 15. FF pattern in the cut plane at $\varphi = 90°$. Solid line: reference. Crosses: reconstructed from nonuniform NF data via the SVD-based algorithm.

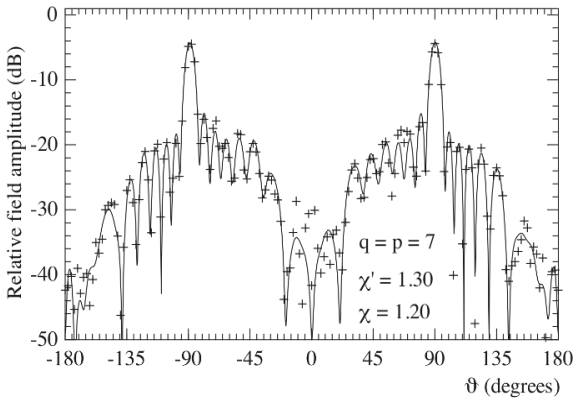

Fig. 16. FF pattern in the cut plane at $\varphi = 90°$. Solid line: reference. Crosses: reconstructed from nonuniform NF data without using the SVD-based algorithm.

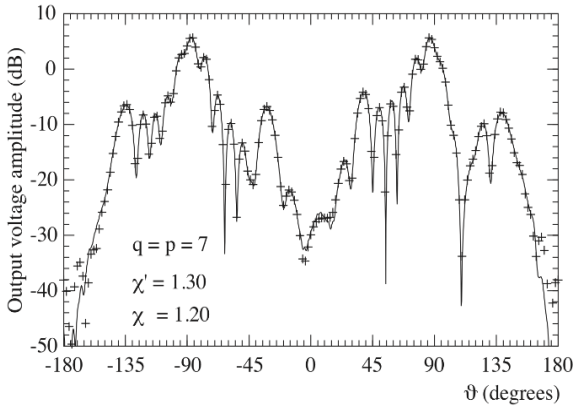

Fig. 17. Amplitude of the voltage V_1 on the meridian at $\varphi = 0°$. Solid line: measured. Crosses: reconstructed from nonuniform NF data via the iterative algorithm.

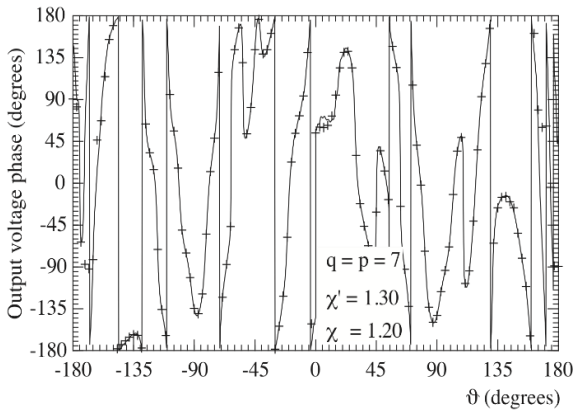

Fig. 18. Phase of V_1 on the meridian at $\varphi = 0°$. Solid line: measured. Crosses: reconstructed from nonuniform NF data via the iterative algorithm.

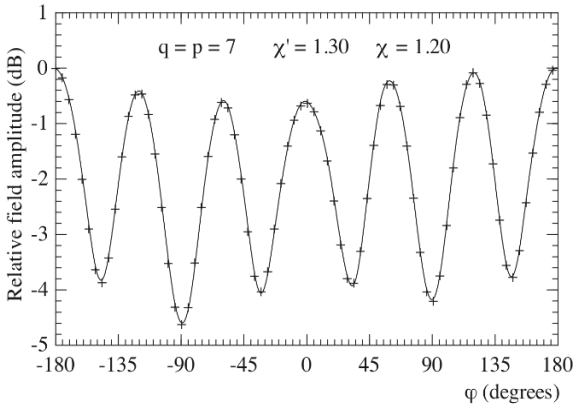

Fig. 19. E-plane ($\vartheta = 90°$) pattern. Solid line: reference. Crosses: reconstructed from nonuniform NF data via the iterative algorithm.

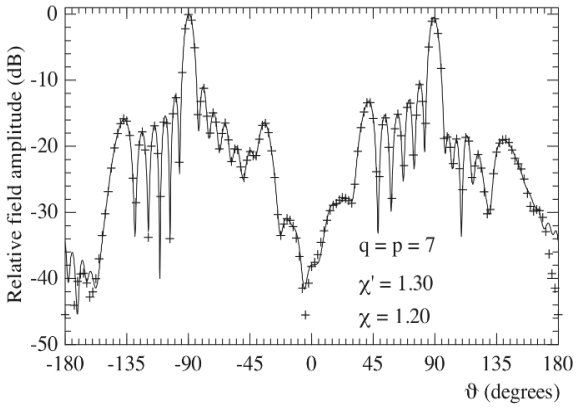

Fig. 20. H-plane ($\varphi = 0°$) pattern. Solid line: reference. Crosses: reconstructed from nonuniform NF data via the iterative algorithm.

VI. CONCLUSION

In this paper, two different efficient techniques, which allow the correction of known positioning errors in the nonredundant spherical NF–FF transformation using the rounded cylinder modelling, have been presented. Both the techniques retrieve the nonredundant uniform NF samples at the points fixed by the sampling representation from the acquired irregularly distributed ones. Then, these retrieved samples are efficiently interpolated via an OSI algorithm to accurately reconstruct the NF data required to perform the classical spherical NF–FF transformation. In order to recover the uniform samples, the former technique makes use of the SVD method and can be profitably employed when the nonuniform samples lie on parallels, so that the uniform samples recovery can be reduced to the solution of two independent one-dimensional problems. The latter adopts an iterative scheme, which does not require the fulfillment of such a hypothesis, but can be applied only if there is a biunique correspondence between each uniform sampling point and the nearest nonuniform one. Some numerical and experimental results assessing the effectiveness of both the techniques, even in presence of large and pessimistic positioning errors in an actual scan, have been shown.

REFERENCES

[1] F. Jensen, *Electromagnetic Near-Field–Far-Field Correlations, Ph.D. Dissertation*, Tech. Univ. of Denmark, Rep. LD15, 1970.

[2] F. Jensen, "On the probe compensation for near-field measurements on a sphere," *Archiv Elektr. Übertr*., vol. 29, pp. 306-308, 1975.

[3] P. F. Wacker, "Non-planar near-field measurements: spherical scanning," *NBSIR 75-809*, Boulder, CO, USA, 1975.

[4] F. H. Larsen, "Probe correction of spherical near-field measurements," *Electr. Lett*., vol. 13, pp. 393-395, July 1977.

[5] F. H. Larsen, *Probe-Corrected Spherical Near-Field Antenna Measurements, Ph.D. Dissertation*, Tech. Univ. of Denmark, Rep. LD36, 1980.

[6] J. Hald, J. E. Hansen, F. Jensen, and F. H. Larsen, *Spherical Near-Field Antenna Measurements*, J. E. Hansen Ed., IEE Electromagnetic Waves Series, Peter Peregrinus, London, UK, 1998.

[7] A. D. Yaghjian, "Simplified approach to probe-corrected spherical near-field scanning," *Electr. Lett*., vol. 20, pp. 195-196, Mar. 1984.

[8] A. D. Yaghjian and R. C. Wittmann, "The receiving antenna as a linear differential operator: application to spherical near-field measurements,"

IEEE Trans. Antennas Prop., vol. AP-33, pp. 1175-1185, 1985.

[9] T. Laitinen, S. Pivnenko, J. M. Nielsen, and O. Breinbjerg, "Theory and practice of the FFT/matrix inversion technique for probe-corrected spherical near-field antenna measurements with high-order probes," *IEEE Trans. Antennas Prop*., vol. 58, pp. 2623-2631, Aug. 2010.

[10] T. B. Hansen, "Numerical investigation of the system-matrix method for higher-order probe correction in spherical near-field antenna measurements," *Int. Jour. Antennas Prop*., vol. 2012, ID 493705, 8 pages, 2012.

[11] O. M. Bucci, F. D'Agostino, C. Gennarelli, G. Riccio, and C. Savarese, "Data reduction in the NF–FF transformation technique with spherical scanning," *Jour. Electr. Waves Appl*., vol. 15, pp. 755-775, 2001.

[12] F. D'Agostino, F. Ferrara, C. Gennarelli, R. Guerriero, and M. Migliozzi, "Non-redundant spherical NF – FF transformations using ellipsoidal antenna modeling: experimental assessments," *IEEE Antennas Prop. Magaz*., vol. 55, pp. 166-175, 2013.

[13] F. D'Agostino, F. Ferrara, C. Gennarelli, R. Guerriero, and M. Migliozzi, "Effective antenna modellings for NF–FF transformations with spherical scanning using the minimum number of data," *Int. Jour. Antennas Prop*., vol. 2011, ID 936781, 11 pages, 2011.

[14] F. D'Agostino, F. Ferrara, C. Gennarelli, R. Guerriero, and M. Migliozzi, "Experimental testing of nonredundant near-field to far-field transformations with spherical scanning using flexible modellings for nonvolumetric antennas," *Int. Jour. Antennas Prop*., vol. 2013, ID 517934, 10 pages, 2013.

[15] M. A. Qureshi, C. H. Schmidt, and T. F. Eibert, "Adaptive sampling in spherical and cylindrical near-field antenna measurements," *IEEE Antennas Prop. Magaz*., vol. 55, pp. 243-249, Feb. 2013.

[16] O. M. Bucci and G. Franceschetti, "On the spatial bandwidth of scattered fields," *IEEE Trans. Antennas Prop*., vol. AP-35, pp. 1445-1455, Dec. 1987.

[17] O. M. Bucci, C. Gennarelli, and C. Savarese, "Representation of electromagnetic fields over arbitrary surfaces by a finite and non redundant number of samples," *IEEE Trans. Antennas Prop*., vol. 46, pp. 351-359, Mar. 1998.

[18] O. M. Bucci and C. Gennarelli, "Application of nonredundant sampling representations of electromagnetic fields to NF-FF transformation techniques," *Int. Jour. Antennas Prop*., vol. 2012, ID 319856, 14 pages, 2012.

[19] A. Dutt and V. Rohklin, "Fast Fourier transforms for nonequispaced data," *Proc. SIAM Jour. Scient. Comp.*, vol. 14, pp. 1369-1393, 1993.

[20] G. Beylkin, "On the fast Fourier transform of functions with singularities," *Appl. Comp. Harmonic Analysis*, vol. 2, pp. 363-381, 1995.

[21] R. C. Wittmann, B. K. Alpert, and M. H. Francis, "Near-field antenna measurements using nonideal measurement locations," *IEEE Trans. Antennas Prop*., vol. 46, pp. 716-722, May 1998.

[22] R. C. Wittmann, B. K. Alpert, and M. H. Francis, "Near-field, spherical-scanning antenna measurements with nonideal probe locations," *IEEE Trans. Antennas Prop*., vol. 52, pp. 2184-2186, Aug. 2004.

[23] O. M. Bucci, C. Gennarelli, and C. Savarese, "Interpolation of electromagnetic radiated fields over a plane from nonuniform samples," *IEEE Trans. Antennas Prop*., vol. 41, pp. 1501-1508, Nov. 1993.

[24] O. M. Bucci, C. Gennarelli, G. Riccio, and C. Savarese, "Electromagnetic fields interpolation from nonuniform samples over spherical and cylindrical surfaces," *IEE Proc. Microw. Antennas Prop*., vol. 141, pp. 77-84, Apr. 1994.

[25] F. Ferrara, C. Gennarelli, G. Riccio, and C. Savarese, "Far field reconstruction from nonuniform plane-polar data: a SVD based approach," *Electromagnetics*, vol. 23, pp. 417-429, 2003.

[26] F. D'Agostino, F. Ferrara, C. Gennarelli, R. Guerriero, M. Migliozzi, and G. Riccio, "A singular value decomposition based approach for far-field reconstruction from irregularly spaced planar wide-mesh scanning data," *Microw. Opt. Tech. Lett*., vol. 49, pp. 1768-1772, July 2007.

[27] F. Ferrara, C. Gennarelli, G. Riccio, and C. Savarese, "NF–FF transformation with cylindrical scanning from nonuniformly distributed data," *Microw. Opt. Tech. Lett*., vol. 39, pp. 4-8, Oct. 2003.

[28] F. D'Agostino, F. Ferrara, C. Gennarelli, R. Guerriero, and M. Migliozzi, "Two techniques for compensating the probe positioning errors in the spherical NF–FF transformation for elongated antennas," *The Open Elect. Electr. Eng. Jour*., vol. 5, pp. 29-36, 2011.

[29] F. D'Agostino, F. Ferrara, C. Gennarelli, R. Guerriero, M. Migliozzi, and D. Spagnuolo, "Compensation of the probe positioning errors in the spherical NF–FF transformation for elongated antennas," *Proc. of ICEAA'11*, pp. 255-258, Turin, Sept. 2011.

Francesco D'Agostino was born near Salerno (Italy) in 1965. He received the Laurea degree in Electronic Engineering from the University of Salerno in 1994, where in 2001 he received the Ph.D. degree in Information Engineering. From 2002 to 2005 he was Assistant Professor at the Engineering Faculty of the University of Salerno where in October 2005, he was appointed Associate Professor of Electromagnetics and joined the Department of Industrial Engineering, where he is currently working. His research activity includes application of sampling techniques to electromagnetics and to innovative NF–FF transformations, diffraction problems radar cross section evaluations, Electromagnetic Compatibility. In this area, D'Agostino has co-authored 4 books and over 150 scientific papers, published in peer-reviewed international journals and conference proceedings. He is a regular Reviewer for several journals and conferences and has chaired some international events and conferences. D'Agostino is a Member of AMTA, EurAAP, and IEEE.

Flaminio Ferrara was born near Salerno, Italy, in 1972. He received the Laurea degree in Electronic Engineering from the University of Salerno in 1999. Since the same year, he has been with the Research Group in Applied Electromagnetics at the University of Salerno. He received the Ph.D. degree in Information Engineering at the same University, where he is presently an Assistant Professor of Electromagnetic Fields. His interests include: application of sampling techniques to the efficient reconstruction of electromagnetic fields and to NF–FF transformation techniques; monostatic radar cross section evaluations of corner reflectors. Ferrara is co-author of more than 180 scientific papers, mainly in international journals and conference proceedings. He is a Member of the IEEE society.

Claudio Gennarelli was born in Avellino, Italy, in 1953. He received the Laurea degree (*summa cum laude*) in Electronic Engineering from the University of Naples, Italy, in 1978. From 1978 to 1983, he worked with the Research Group in Electromagnetics at the Electronic Engineering Department of the University "Federico II" of Naples. In 1983, he became Assistant Professor at the Istituto Universitario Navale (IUN), Naples. In 1987, he was appointed Associate Professor of Antennas, formerly at the Engineering Faculty of Ancona University and subsequently at the Engineering Faculty of Salerno University. In 1999, he has been appointed Full Professor at the same University. The main topics of his scientific activity are: reflector antennas analysis, antenna measurements, diffraction problems, radar cross section evaluations, scattering from surface impedances, application of sampling techniques to electromagnetics and to NF–FF transformations. Gennarelli is co-author of more than 360 scientific papers, mainly in international journals and conference proceedings. In particular, he is co-author of four books on NF–FF Transformation Techniques. He is a Senior Member of the IEEE and Member of the Editorial board of the Open Electrical and Electronic Engineering Journal and of the International Journal of Antennas and Propagation.

Rocco Guerriero received the Laurea degree in Electronic Engineering and the Ph.D. degree in Information Engineering from the University of Salerno in 2003 and 2007, respectively. Since 2003, he has been with the Reaserch Group in Applied Electromagnetics of University of Salerno, where he is currently an Assistant Professor of Electromagnetic Fields. His interests include: application of sampling techniques to the efficient reconstruction of electromagnetic fields and to near-field-far-field transformation techniques; antenna measurements; inversion of ill-posed electromagnetic problems; analysis of microstrip reflectarrays; diffraction problems. Guerriero is co-author of more than 135 scientific papers, mainly in international journals and conference proceedings. Since 2015, he is a Member of IEEE.

Massimo Migliozzi received the Laurea degree in Electronic Engineering from the University of Salerno, in 1999. He received the Ph.D. degree in Information Engineering at the same University, where at the present time he is a Research fellow in Electromagnetic Fields. His scientific interests include: application of sampling techniques to the efficient reconstruction of electromagnetic fields and to NF–FF transformation techniques; antenna measurements; electromagnetic compatibility; antenna design; diffraction problems. Migliozzi is co-author of about 100 scientific papers, mainly in international journals and conference proceedings.